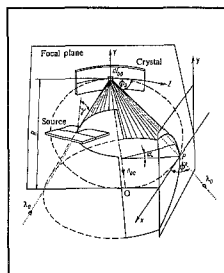


A. Meisel, Karl-Marx-Universität, Leipzig; G. Leonhardt, TU Karl-Marx-Stadt; R. Szargan, Karl-Marx-Universität, Leipzig

X-Ray Spectra and Chemical Binding



1989. VIII, 458 pp. 228 figs.
(Springer Series in Chemical Physics,
Volume 37) Hardcover DM 198,-
ISBN 3-540-13325-9

This book focuses on the relation between X-ray spectra and the electronic structure of matter. Discussions of the physical processes are combined with interpretation of spectra from the perspective of chemistry to give a unified and rigorous presentation that makes considerable use of chemical intuition and recognizes intrinsic complexities such as incomplete relaxation and multivacancy production. The authors review experimental methods, results and analyses, and apply the results to chemistry, materials science and the electronic structure of matter. The extensive bibliography facilitates access to primary literature.

Springer-Verlag
Berlin Heidelberg
New York
London Paris
Tokyo Hong Kong

Heidelberger Platz 3,
D-1000 Berlin 33 · 175 Fifth Ave.,
New York, NY 10010, USA ·
8 Alexandra Rd., London SW19
7JZ, England · 26, rue des Carmes,
F-75005 Paris · 37-3, Hongo
3-chome, Bunkyo-ku, Tokyo 113,
Japan · Citicorp Centre,
Room 1603, 18 Whitfield Road,
Causeway Bay, Hong Kong

Springer



tm. 9229/14/4h

FORTHCOMING PAPERS

Frequency Stability of an Optically Pumped Cesium Beam Frequency Standard

V. Candelier, V. Giordano, A. Hamel, G. Théobald, P. Cérez, C. Audoin (France)

Results obtained in an experimental optically pumped cesium beam frequency standard in which a single semiconductor laser is used for the state selection and the atom detection are reported. The separation between the two interaction regions is equal to 21 cm. This gives a 500 Hz linewidth which is observed with a signal to noise ratio equal to 10 000 in a 1 Hz noise bandwidth. A quartz crystal oscillator is frequency controlled by the atomic transition. The measured short term frequency stability is given by $\sigma_y(\tau) = 2 \times 10^{-12} \tau^{-1/2}$ for $1 \text{ s} < \tau \lesssim 500 \text{ s}$. Prospects for improvement of this frequency stability are discussed.

Doppler-Free Resonances of the Second-Order Raman Scattering

V. P. Chebotayev, V. A. Ulybin (USSR)

The possibility of the observation of Raman scattering resonances completely free from the influence of the Doppler effect has been examined for the first time. The phenomenon is based on the excitation of a Raman oscillation standing wave in a gas by two standing light waves, whose frequency difference is equal to half the Raman frequency. The complete compensation of Doppler shifts results from the simultaneous interactions between atomic particles and two pairs of counter-propagating waves. Doppler-free resonances of the second-order Raman light scattering appear in the number of particles excited to the upper Raman level and in the radiation at the Stokes and anti-Stokes frequencies. The amplitude estimate for the resonance in the number of particles is given for the example of neon.

Dynamics of Laser-Induced Bubble and Free-Surface Oscillations in Absorbing Liquid

V. Yu. Bazhenov, M. V. Vasnetsov, M. S. Soskin, V. B. Taranenko (USSR)

A series of laser-driven dynamic photocapillary effects in absorbing liquid are described. We have observed self-oscillations of the free surface of a liquid (iodine solution in ethanol) and laser-induced bubble trapping and oscillations excited by a low power cw argon laser.

Pulsed 469.4 nm Hollow Cathode He-Kr Laser

M. Jánossy, K. Rózsa, P. Apai, P. Mezei, P. Horváth, L. Csillag, N. Kroó (Hungary)

Design principles, construction and operation characteristics of a pulsed 469.4 nm He-Kr laser are described. The laser was operated in a 20 cm active length transverse hollow cathode discharge and was excited by 50 Hz repetition rate 0.1—1 ms duration square wave current pulses. Cathodoresis of Kr ions was found to play an important role in forming the laser pulse shape. By increasing the voltage a considerable increase of peak laser power occurred, the maximum power obtained was 80 mW. The sealed-off laser was operated using 400 μs , 4 A current pulses, pulsed laser power being 20 mW, average power 0.4 mW, respectively. The lifetime of the laser was 440 h, tube failure being due to gas clean-up caused by cathode sputtering.

Atmospheric Influences in Optical Third-Harmonic Generation Experiments

F. Krausz, E. Wintner (Austria)

Third-harmonic generation in a thin solid plate surrounded by a gas is investigated. We conclude that atmospheric contributions can be suppressed in third-harmonic generation from thin solid plates. A phase-sensitive measurement of the third-order susceptibility of gases is proposed. We calibrated the third-order susceptibility of air to be $\chi_a^{(3)} = (3.4 \pm 1.5) \times 10^{-18}$ esu with a phase uncertainty of $\pm 10^\circ$.

Applied Physics A 49, No. 3 (1989)

Solids and Materials

J. Faber, C. Geoffroy, A. Roux, A. Sylvestre, P. Abélard
A Systematic Investigation of the dc Electrical Conductivity of Rare-Earth Doped Ceria 225

A. Barhdadi, H. Amzil, J. C. Muller, P. Siffert
Thermal Annealing Effects on Grain Boundary Recombination Activity in Silicon 233

S. W. Martin
Conductivity Relaxation in Glass: Compositional Contributions to Non-Exponentiality 239

M. Cole, M. H. Sheldon, M. D. Glasse, R. J. Latham, R. G. Linford
EXAFS and Thermal Studies on Zinc Polymeric Electrolytes 249

R. A. Rupp, A. Maillard, J. Walter
Impact of the Sublinear Photoconductivity Law on the Interpretation of Holographic Results in BaTiO₃ 259

D. Czekaj, E. K. Hollmann, A. B. Kozirev, V. A. Volpyas, A. G. Zaytsev
Ion Energies at the Cathode of the DC Planar Magnetron Sputtering Discharge 269

M. A. Angadi, K. Nallamshetty
Electrical Conduction in Cu/Mn Multilayer Films 273

Surfaces, Interfaces and Layer Structures

J. Kempf, M. Nonnenmacher, H. H. Wagner
Photoexcitation of Electron-Hole Pairs During SIMS 279

C. S. Fang, Y. L. Chang, W. S. Tse
Effects of Annealing Temperature on the Alloying Behaviour of the AuGe—GaAs(100) Interface 285

R. I. Hornsey
The Emission Characteristics of an Indium Needle-Type Liquid Metal Ion Source 293

A. I. Dodonov, I. M. Fayazov, S. D. Fedorovich, E. A. Krylova, E. S. Maskova, V. A. Molchanov, W. Eckstein
Experimental and Computer Study of the Spatial Distributions of Particles Sputtered from Polycrystals 299

T. Kanata, H. Takakura, Y. Hamakawa
Preparation of Composition-Controlled Silicon Oxynitride Films by Sputtering; Deposition Mechanism, and Optical and Surface Properties 305

H. Hinzert, K. K. Kleinherbers, E. Janssen, A. Goldmann
Chemisorption of Halogens on Silver. A Critical Comparison of Results from Photoemission and Thermal Desorption Spectroscopy 313

W. C. Liu, W. S. Lour, C. Y. Chang
Application of Superlattice Gate and Modulation-Doped Buffer for GaAs Power MESFET Grown by MBE 321

Rapid Communication

R. E. DeWames, P. E. D. Morgan, J. J. Ratto, J. R. Porter, W. F. Hall, D. B. Marshall, I. B. Goldberg
Remanent Fields and Critical Currents in Ti₂Ba₂Ca₂Cu₃O_x Ceramic 325

S. C. Gadkari, K. P. Muthe, K. D. Singh, S. C. Sabharwal, M. K. Gupta
Preparation of Bi—Sr—Ca—Cu—O Bulk Superconductor and Thick Films 331

T. E. Jackman, G. C. Aers, M. W. Denhoff, P. J. Schultz
Point-Defect Production in Arsenic-Doped Silicon Studied with Variable-Energy Positrons 333